

A CONE MODEL FOR CORONAL MASS EJECTIONS

W. Liu¹, S. P. Plunkett², X. P. Zhao¹

¹*W. W. Hansen Experimental Physics Laboratory, Stanford University, Stanford, CA 94305-4085, USA*

²*University Space Research Association, Naval Research Laboratory, Code 7660, Washington, DC 20375, USA*

ABSTRACT

As an extension of the previous study (Zhao *et al.*, 2001, hereafter Paper I), the cone model for coronal mass ejections (CMEs) is applied to more events to infer their geometrical and kinematical properties in an effort to measure the line-of-sight speed of front-side halo CMEs and determine their geoeffectiveness. It turns out that this model is quite applicable to a variety of CMEs. By incorporating projection effects in detail, the cone model holds the potential of providing the real line-of-sight speed of halo CMEs. Based on this model, a more quantitative estimate is proposed to determine the range of the orientation for a CME to form a visible halo.

INTRODUCTION

Halo CMEs have been interpreted as broad shells or bubbles of dense plasma ejected directly toward (or away from) the Earth. The line-of-sight speed of front-side halo CMEs, associated with their geometrical and kinematical properties, is one of the key parameters that determine the geoeffectiveness of CMEs. However, there were relatively few systematic studies of the correlation between the projection effects and geometrical properties of halo CMEs (e.g., Sheeley *et al.*, 1999). Aiming to fill this gap, a cone model has been developed to help determine the line-of-sight speed of halo CMEs, based on the fact that many CMEs are observed to propagate radially and have constant angular widths (Paper I and references therein). In the present paper, we will test the applicability of the cone model by examining more examples and improve our estimate of the occurrence of halo CMEs in a more quantitative manner.

APPLICATION OF THE CONE MODEL

In Paper I, we modeled the boundary of emission of a halo CME observed by LASCO with a cone that has a constant angular spread ω , with its apex located at the center of the Sun and its central axis running through the CME source location (specified by the latitude λ and longitude ϕ measured from the central meridian passing). Then, a modeled CME halo can be reproduced with the projection of the round cross section of the cone at a specific radial distance r on the sky plane. The angular width ω and orientation (λ and ϕ) of the cone can be determined by matching the modeled halo at a distance r with the observed one at the corresponding time. Finally, the radial speed (also the line-of-sight speed) and acceleration can be inferred by matching a series of halo CME images at separate times. This model has been applied to obtain the geometrical and kinematical properties of the 1997 May 12 halo CME (Paper I).

To further test its applicability, the 1999 Aug. 17 partial halo CME (first seen in C2 at 14:06:06 UT) is analyzed using the cone model. The results are shown in Figure 1, where the black curves (over-plotted on coronagraph images) are the projections of the cross sections of the cone obtained with an angular width $\omega = 60^\circ$, longitude $\phi = -20^\circ$, and latitude $\lambda = 23^\circ$, at different radial distances. A plot of radial distance v.s. time is shown in Figure 2, in which the fitting is performed by minimizing the maximum error (Paper I and references therein). The solid (dotted) line in the top panel is the constant-acceleration (constant-speed) fitting to the scatter points. The bottom panel of Figure 2 displays the inferred radial speed at various heliocentric distances, showing an acceleration with the speed changing from 714 km/s at 8.1 solar radii to 1080 km/s at 32.3 solar radii for the constant-acceleration fitting curve. Further more, this cone

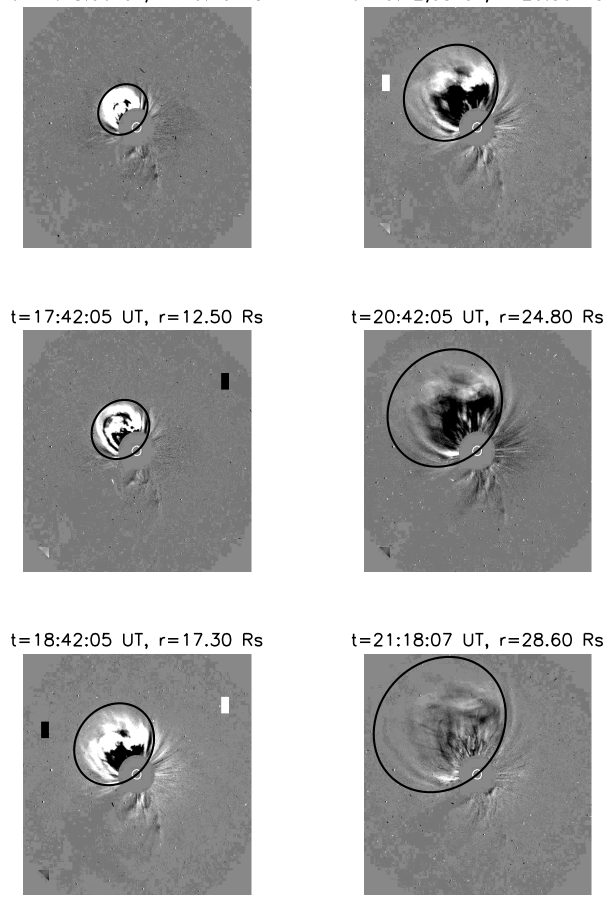


Fig. 1. Comparison of the modeled halos (in black) at different radial distances (in solar radii) with the observed ones at the corresponding times for the 1999 Aug. 17 partial halo CME. The cone parameters are $\omega = 60^\circ$, $\phi = -20^\circ$, and $\lambda = 23^\circ$.

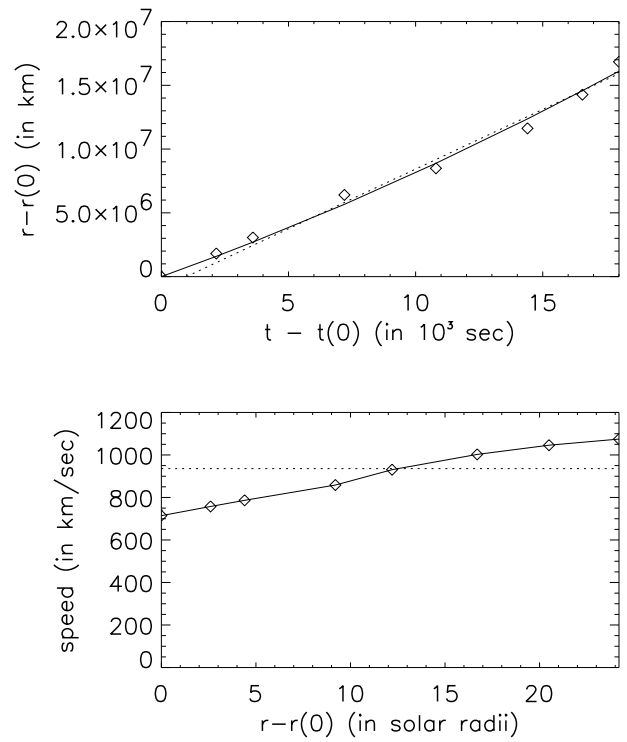


Fig. 2. (a) Top panel: the plot of the inferred series of time and radial distance for the 1999 Aug. 17 partial halo CME. $r(0)$ and $t(0)$ are, respectively, the radial distance 8.1 solar radii and the time 16:42:05 UT. The solid (dotted) line is the fitting curve obtained using the constant-acceleration (constant-speed) fitting. (b) Bottom panel: the radial speed at various heights inferred from the above fitting, with the same meaning of the solid and dotted lines.

model is applied to a number of typical CMEs with the results summarized in Table 1, demonstrating its applicability to a large variety of CMEs (including full halo, partial halo, and even limb events).

DEPENDENCE OF HALO CME OCCURRENCE ON ORIENTATION & ANGULAR WIDTH

What should the range of the orientation be for a CME with an angular width of ω to form a visible halo? In Paper I, we proposed that for halo CMEs with an angular width of 45° , the source location is located within a circle of $\sim 15^\circ$ from the center of solar disk, and for partial halo CMEs, it is located between 15 and 30 degrees from the disk center. As a matter of fact, the visibility of halo CMEs depends on many factors, such as the radial distance from the Sun, the projection angle from the sky plane, the coronal electron density distribution, and the dependence of Thomson-scattering intensity on these factors (refer to Plunkett *et al.*, 1998 in References of Paper I). To make a rough but more quantitative estimate, we take the liberty to assume the visibility of a halo CME merely depends on its radial distance r from the solar center and there exists an upper limit r_{max} for a CME to be visible. Meanwhile, a CME must appear as a ring at least in the C2 field of view to form a visible halo. Therefore, given the cone's angular width ω , to produce a visible halo using the cone model, the upper limit of the angle of the cone's central axis from the disk center, α_{max} , can be expressed as $\alpha_{max} = \omega/2 - \beta_{min}$, where $\beta_{min} = \arcsin(R_0/r_{max})$ is the minimum angle between the line of sight and the edge of the cone on the same side of the axis and R_0 ($=2$ solar radii) the radius of the occulting disk of C2 (Figure 3). Figure 4 shows the dependence of α_{max} on ω and r_{max} , with each curve corresponding to a value of r_{max} . As r_{max} increases, the above equation for α_{max} approaches the limiting case of $\alpha_{max} = \omega/2$, with decreasing separations between the curves as shown in the figure. For instance, taking $r_{max} \sim 45$ solar radii (1.5 times the radius of the C3 field of view) and

Table 1. Geometrical and kinematical properties of typical CMEs. (\bar{v} : the mean radial speed obtained with the constant-speed fitting; v_0 and a : initial speed and acceleration inferred from the constant-acceleration fitting.)

| Events | $\omega(^{\circ})$ | $\phi(^{\circ})$ | $\lambda(^{\circ})$ | \bar{v} (km/s) | v_0 (km/s) | $a(10^{-2} \text{ km/s}^2)$ | CME types |
|-----------|--------------------|------------------|---------------------|------------------|--------------|-----------------------------|--------------|
| 01/06/97 | 63 | 2.4 | -3 | 362 | 308 | 0.402 | full halo |
| 06/30/99 | 65.5 | 6.5 | 5.5 | 1160 | 1410 | -3.14 | full halo |
| 08/17/99 | 60 | -20 | 23 | 936 | 714 | 2.00 | partial halo |
| 10/13/99 | 40 | -15 | 55 | 563 | 361 | 1.55 | limb event |
| 02/17/00 | 92 | 5 | -5 | 517 | 832 | -4.12 | full halo |
| 07/14/00 | 46 | 3 | 3.2 | 2080 | 2360 | -15.8 | full halo |
| 09/12/00 | 71 | 1 | -10 | 1350 | 1460 | -1.19 | full halo |
| 11/24b/00 | 61 | 8 | 6 | 1140 | 1290 | -1.75 | full halo |
| 11/26b/00 | 58 | 8 | 3 | 1290 | 1610 | -6.06 | full halo |

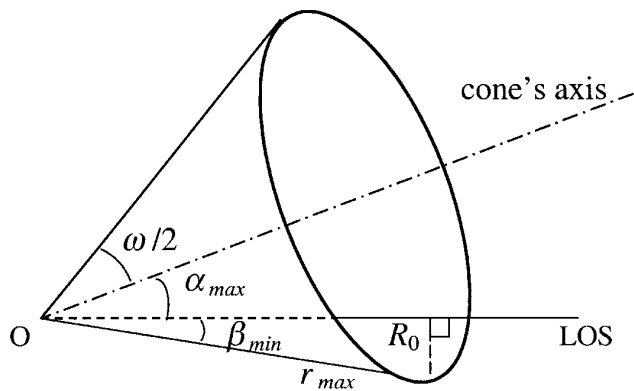


Fig. 3. Geometry to estimate the range of orientation for a cone-like CME to form a visible halo. "LOS" refers to the line of sight; "O" the solar center; $\omega/2$ the half angular width of the cone; α_{max} the largest deviation of the cone's axis from LOS; β_{min} the minimum angle between LOS and the edge of the cone on the same side of the axis.

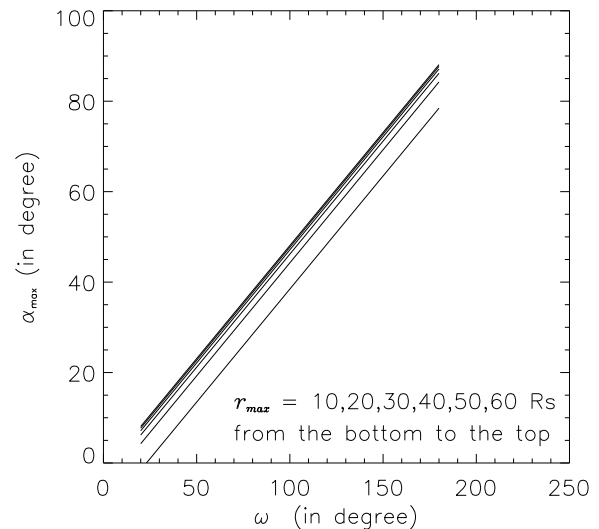


Fig. 4. Dependence of α_{max} on ω and r_{max} , as described by $\alpha_{max} = \omega/2 - \arcsin(R_0/r_{max})$ in the text.

$\omega \sim 45^{\circ}$ (the average limb CME angular width), we have $\alpha_{max} \sim 20^{\circ}$, which gives the range of the cone's orientation to be within a circle of $\sim 20^{\circ}$ from the disk center.

SUMMARY AND DISCUSSION

The cone model (Paper I) has been further applied to a variety of CMEs to test its applicability. It turns out that this model has the potential of providing geometric and kinematical properties of halo CMEs and inferring their line-of-sight speed. We also present a semi-quantitative criterion for a CME with a given angular width to form a visible full halo. However, there are several issues needed to be explored more extensively. First, the cone solution is degenerate when the central axis of the cone is aligned with the line of sight (Paper I). This stems from the fact that only the information in the 2-D sky plane is included in the study. Therefore, it is necessary to retrieve other information from the third dimension which could be provided with radio or stereo observations. Second, there exists uncertainty in identifying and matching the outer edge of rather fuzzy halo CMEs. We expect to find a better method to make the otherwise fuzzy halos easier to be identified and set a rather objective criterion that determines the optimal matching.

REFERENCES

- Sheeley, N. R., Jr., J. H. Walters, Y. M. Wang, and R. A. Howard, Continuous Tracking of Coronal Outflows: Two Kinds of Coronal Mass Ejections, *J. Geophys. Res.*, **104**, 24739 (1999).
- Zhao, X. P., S. P. Plunkett, and W. Liu, Determination of Geometrical and Kinematical Properties of Halo Coronal Mass Ejections Using the Cone Model, submitted to *J. Geophys. Res.* (2001) (Paper I).